Title
Comparison of loading rate-dependent injury modes in a murine model of post-traumatic osteoarthritis.

Permalink
https://escholarship.org/uc/item/2m93g2xt

Journal
Journal of orthopaedic research : official publication of the Orthopaedic Research Society, 32(1)

ISSN
0736-0266

Authors
Lockwood, Kevin A
Chu, Bryce T
Anderson, Matthew J
et al.

Publication Date
2014

DOI
10.1002/jor.22480

Peer reviewed

Comparison of loading rate-dependent injury modes in a murine model of post-traumatic osteoarthritis

Kevin A. Lockwood, M.S., **Bryce T. Chu, B.S.**, **Matthew J. Anderson, M.S.**, **Dominik R. Haudenschild, Ph.D.**, and **Blaine A. Christiansen, Ph.D.**
University of California – Davis Medical Center, Sacramento, CA

Abstract

Post-traumatic osteoarthritis (PTOA) is a common long-term consequence of joint injuries such as anterior cruciate ligament (ACL) rupture. In this study we used a tibial compression overload mouse model to compare knee injury induced at low speed (1 mm/s), which creates an avulsion fracture, to injury induced at high speed (500 mm/s), which induces midsubstance tear of the ACL. Mice were sacrificed at 0 days, 10 days, 12 weeks, or 16 weeks post-injury, and joints were analyzed with micro-computed tomography, whole joint histology, and biomechanical laxity testing. Knee injury with both injury modes caused considerable trabecular bone loss by 10 days post-injury, with the Low Speed Injury group (avulsion) exhibiting a greater amount of bone loss than the High Speed Injury group (midsubstance tear). Immediately after injury, both injury modes resulted in greater than 2-fold increases in total AP joint laxity relative to control knees. By 12 and 16 weeks post-injury, total AP laxity was restored to uninjured control values, possibly due to knee stabilization via osteophyte formation. This model presents an opportunity to explore fundamental questions regarding the role of bone turnover in PTOA, and the findings of this study support a biomechanical mechanism of osteophyte formation following injury.

Keywords

Mouse model; Post-traumatic osteoarthritis; ACL injury; Joint stability; Osteophyte

INTRODUCTION

Osteoarthritis (OA) is the most common joint disease, and the knee is the most commonly affected joint [1]. OA causes pain and stiffness in the joint, and severely limits mobility for those people who are affected. Current evidence indicates that after non-contact anterior cruciate ligament (ACL) injury, patients have an increased chance of developing post-traumatic osteoarthritis (PTOA) within 10–20 years after injury [2, 3].

Animal models are useful tools for studying PTOA, since the disease process can be studied in a more controlled environment on a dramatically condensed time line. There have been a

number of mouse models developed for studying PTOA [4–7], but many of these still have significant drawback such as invasive surgery or multiple bouts of mechanical loading. Our lab has developed a non-invasive mouse model that induces ACL rupture in mice *in vivo* by a single tibial compression overload [8]. This model closely mimics traumatic ACL rupture in humans without the costs and complications of surgery.

Our previous study using this mouse model had limitations, including ACL damage primarily by avulsion fractures rather than midsubstance tears, induction of only mild osteoarthritis by the end of the study (8 weeks post-injury), and little quantification of joint biomechanics [8]. Avulsion fracture is not a common injury mode in adults [9], therefore a more clinically relevant mouse model would induce a midsubstance tear of the ACL rather than failure by an avulsion fracture. Based on the results from Crowninshield et al. [10] and Noyes et al. [11], we hypothesized that increasing the loading rate during knee injury would cause midsubstance ACL tears and decrease the likelihood of an avulsion fracture.

In this study we used our non-invasive mouse injury model to compare biomechanical and structural changes in the joint following ACL injury either with avulsion fracture or with midsubstance tear. We examined short term (10 days) and long term (12–16 weeks) structural changes in subchondral bone and epiphyseal trabecular bone, osteophyte formation, articular cartilage degeneration, and biomechanical stability of injured vs. uninjured knees. We hypothesized that injury mode (avulsion vs. midsubstance tear) would not significantly affect structural bone changes, osteoarthritis development, or biomechanical stability.

METHODS

Animals

A total of 80 male C57BL/6N mice (10 weeks old at time of injury) were obtained from Harlan Sprague Dawley, Inc. (Indianapolis, IN). Mice underwent a one-week acclimation period in a housing facility before injury. Mice were caged individually and were maintained and used in accordance with National Institutes of Health guidelines on the care and use of laboratory animals. All procedures were approved by our Institutional Animal Care and Use Committee.

Non-Invasive Knee Injury

ACL injury was induced as previously described [8]. Briefly, mice were anesthetized using isoflurane inhalation, then the right lower leg was positioned between two loading platens: an upper platen that held the flexed ankle at approximately 30 degrees of dorsiflexion and a lower platen that held the flexed knee. The platens were aligned vertically in an electromagnetic materials testing machine (Bose ElectroForce 3200, Eden Prairie, MN). A preload of 1 N was applied to the knee before a single dynamic axial compressive load was applied to a target displacement of −1.7 mm at a loading rate of either 1 mm/s or 500 mm/s. A target displacement was chosen rather than a target compressive load (as in our previous study) to minimize overshoot at high loading rates. Compressive loads at ACL rupture were comparable for both 1 mm/s and 500 mm/s loading rates, and were similar to those observed

in our previous study (8–12 N). After injury, mice were given a subcutaneous injection of buprenorphine (0.5 mg/kg body weight) for analgesia. Mice were allowed normal cage activity until sacrifice.

Characterization of Joint Injury—To determine the effect of tibial compression loading rate on injury mode (avulsion fracture vs. midsubstance tear), both knees of 6 mice were injured at loading rates of 10 or 500 mm/s (n = 6 knees per group). Immediately following injury, mice were sacrificed and injured knees were imaged with micro-computed tomography (μCT) as described below to detect the presence of bone fragments in the joint space indicative of avulsion fracture. To further characterize the injuries induced by High Speed or Low Speed tibial compression loading rate, both knees of 10 mice were injured using 1 mm/s (n = 7 knees) or 500 mm/s (n = 7 knees) loading rates, or left intact (n = 6 knees). Mice were sacrificed immediately after injury. Contrast enhanced μCT was performed on six knees (n = 2 per group). Knees were stained with phosphotungstic acid (PTA; 0.3% in 70% ethanol) for one week before being scanned with μCT (2 μm nominal voxel size, Micro Photonics Inc., Allentown, PA). The remaining 14 knees (n = 4–5 per group) were decalcified, sectioned in the sagittal plane, and stained with hematoxylin and eosin (H&E) to assess joint structure.

Comparison of High Speed and Low Speed Injury Models

<u>Study Design:</u> A total of 64 mice were used for this study (Table 1). Half of the injured mice were injured with the 1 mm/s load rate (Low Speed injury; n = 26); the other half were injured with the 500 mm/s load rate (High Speed injury; n = 26). An additional 12 mice underwent sham injury (anesthetized and loaded with the 1 N preload only). Following injury, mice were immediately sacrificed (n = 12) or returned to normal cage activity for 10 days (n = 22), 12 weeks (n = 15), or 16 weeks (n = 15), at which point they were euthanized by CO_2 asphyxiation and both hind limbs were excised for analysis. The left limb served as an internal control for each mouse.

Micro-Computed Tomography of Distal Femoral Epiphysis, Tibial Subchondral Bone, and Osteophytosis

Injured and uninjured knees were imaged with micro-computed tomography (SCANCO μCT 35, Bassersdorf, Switzerland) to quantify trabecular bone structure in the distal femoral epiphysis, subchondral bone structure at the proximal tibia, and osteophyte formation around the joint. Dissected limbs were fixed in 4% paraformaldehyde for 24–48 hours, then transferred to 70% ethanol. Knees were scanned according to the guidelines for micro-computed tomography (μCT) analysis of rodent bone structure [12] (energy = 55 kVp, intensity = 114 mA, 10 μm nominal voxel size, integration time = 900 ms). Trabecular bone in the distal femoral epiphysis was analyzed by manually drawing contours on 2D transverse slices. The distal femoral epiphysis was designated as the region of trabecular bone enclosed by the growth plate and subchondral cortical bone plate. We quantified trabecular bone volume per total volume (BV/TV), trabecular thickness (Tb.Th), trabecular number (Tb.N), and apparent bone mineral density (Apparent BMD; mg HA/cm^3 TV) using the manufacturer's analysis tools. In our previous study [8] we observed comparable trabecular bone changes at the femoral epiphysis, tibial epiphysis, and tibial metaphysis following knee

injury. The current study investigated only the femoral epiphysis, since it has the largest volume for analysis and therefore will yield the most consistent trabecular bone parameters. Subchondral bone of the proximal tibial plateau was analyzed for 12- and 16-week knees. The subchondral bone was segmented for 500 μm (50 slices) distal to the most proximal point of the tibia, excluding the trabecular bone compartment and any osteophytes growing from the tibia. We quantified cortical thickness (Ct.Th) and bone mineral density (BMD; mg HA/cm^3 BV) of the subchondral bone using the manufacturer's analysis tools. We investigated only the tibial suchondral bone because analysis of the subchondral bone of the femoral condyles is technically challenging, as is highly dependent on the orientation of the femur in the μCT scan. Osteophyte volume was calculated for 12- and 16-week knees, and included all mineralized tissue in and around the joint space, excluding naturally ossified structures (patella, fabella, and anterior and posterior horns of the menisci).

Anterior-Posterior Joint Laxity

We quantified joint laxity of injured and uninjured mouse knees using a laxity tester based on previous designs [13, 14]. This tester was designed to interface with a materials testing machine (Bose ElectroForce 3200, Eden Prairie, MN). The protocol was similar to that described by Blankevoort et al. [14] for anterior-posterior (AP) laxity. Briefly, after fixation in brass tubes with polymethyl methacrylate (PMMA), the right and left knees of mice at day 0 (n = 12), week 12 (n = 15), and week 16 (n = 15) after injury were tested at 30°, 60°, and 90° of flexion. For each joint angle, knees underwent five loading cycles to a target force of ±1.5 N at a rate of 0.5 mm/s (Fig. 7). The force was applied normal to the longitudinal axis of the tibia. The femur was fixed during testing, but the tibia was allowed to translate and rotate about its longitudinal axis, giving the system three degrees of freedom of motion. Similar to Blankevoort et al., total AP joint laxity was computed based on the difference between displacement at +0.8 N and −0.8 N.

To assess whether fixation in 4% paraformaldehyde and 70% ethanol had an effect on joint laxity, day 0 limbs were tested fresh-frozen, and then retested after being fixed in 4% paraformaldehyde and preserved in 70% ethanol for 4 weeks. Fixed limbs were allowed to rehydrate in a bath of phosphate buffered saline (PBS) for 3 minutes before potting and testing. During testing, the limbs were continuously hydrated with PBS.

Long Term Whole Joint Histology

Knees were analyzed with whole joint histology to determine the extent of articular cartilage degeneration. Intact joints were decalcified for four days in 10% buffered formic acid and then processed for standard paraffin embedding. For each limb, 6–7 sagittal sections (6 μm thickness) were cut across the entire joint separated by 250 μm. Slides were stained with Safranin-O and Fast Green to assess articular cartilage and other joint structures (meniscus, subchondral bone, osteophytes, etc.). Slides were blinded and graded by four independent readers using the semi-quantitative OARSI scale described by Glasson et al. [15]. Grades were assigned to the medial and lateral tibial plateau, and medial and lateral femoral condyles.

Statistical Analysis

Trabecular bone μCT results for High Speed and Low Speed injury modes were compared at each time point by calculating the difference between injured and uninjured knees for each mouse (injured – uninjured) and using analysis of variance (ANOVA) to compare between groups. Joint laxity of uninjured control (UIC), 1 mm/s, and 500 mm/s injury rate joints were compared at each time point using one-way ANOVA. Differences in joint laxity as a function of knee flexion angle were compared using repeated measures ANOVA. Histology OARSI scores of uninjured control, 1 mm/s, and 500 mm/s injured knees were averaged between readers for each slide, then for all slides for each mouse, and were then compared using one-way ANOVA for each joint region (medial femur, medial tibia, lateral femur, lateral tibia). Significance was defined as $p < 0.05$ for all tests. Mean ± standard deviation is presented for all data.

RESULTS

Characterization of Joint Injury

Non-invasive injury of mice using tibial compression overload with increasing loading rates yielded observable differences in injury mode at the high speed loading rate (500 mm/s) compared to the low speed loading rate (1 mm/s). Using μCT imaging of injured mouse knees, we were able to observe bone fragments indicative of avulsion fracture for all mice injured at 1 mm/s, but we observed no bone fragments at a loading rate of 500 mm/s. We concluded that "High Speed injury" at 500 mm/s caused midsubstance disruption of the ligament, while "Low Speed injury" at 1 mm/s caused a combination injury involving ligament disruption with avulsion fracture. Contrast-enhanced μCT and whole joint histology both showed disruption of the ACL for both 1 mm/s and 500 mm/s injury rates, with no obvious damage to the posterior collateral ligament, menisci, or other structures of the joint (Fig. 1). Consistent with our hypothesis, Low Speed injury (1 mm/s) caused disruption of the ACL with an avulsion fracture from the posterior femur. High Speed injury (500 mm/s) resulted in disruption of the ACL only, with no evidence of avulsion fracture.

Comparison of High Speed and Low Speed Injury Models

Micro-Computed Tomography of Distal Femoral Epiphysis, Tibial Subchondral Bone, and Osteophytosis—Both injury modes initiated a rapid loss of epiphyseal trabecular bone in the distal femur by 10 days post-injury, and long-term joint degeneration and osteophytosis by 12 and 16 weeks post-injury. At all time points, knees injured with either the High Speed or Low Speed loading rates had significantly reduced trabecular BV/TV at the femoral epiphysis compared to uninjured contralateral knees and uninjured control (UIC) mice (Fig. 2). At 10 days post-injury, knees injured using the Low Speed loading rate had significantly greater loss of trabecular BV/TV compared to those injured with the High Speed loading rate (−31% vs. −20%, respectively). By 12 and 16 weeks post-injury, there were no differences in trabecular BV/TV between the High Speed and Low Speed injury modes, although BV/TV of injured knees remained significantly lower than contralateral knees (p < 0.05). At 12 weeks post-injury, BV/TV of High Speed and Low Speed injured knees was 20.9% and 19.6% lower than contralateral knees, respectively, while at 16 weeks, BV/TV of injured knees was 22.9% and 21.5% lower,

respectively. Trabecular thickness (Tb.Th) and apparent bone mineral density (BMD) of the femoral epiphysis followed a similar pattern, with the Low Speed injury rate exhibiting a significantly lower thickness and apparent BMD than the High Speed injury rate at 10 days. At 12 and 16 weeks there were no significant differences between injury modes, but injured limbs had reduced Tb.Th and BMD compared to uninjured contralateral limbs.

Analysis of subchondral bone at the proximal tibia revealed significant thickening of the subchondral bone plate in injured knees by 12 and 16 weeks post-injury (Fig. 3). Cortical thickness was 20–26% larger for injured knees compared to contralateral knees for both injury modes and both time points ($p < 0.05$). However, we observed no significant differences in cortical thickness increase between time points or between injury modes. Bone mineral density of the subchondral bone plate was significantly higher for Low Speed injured knees compared to contralateral knees at week 12 only (908.7 vs. 891.7 mg HA/cm^3; $p = 0.001$). No significant differences in subchondral bone BMD were observed for High Speed injured knees or for any knees at 16 weeks post-injury.

Injured knees exhibited significant osteophytosis using both the High Speed and Low Speed injury modes by 12 and 16 weeks post-injury (Fig. 4–6). The pattern of osteophyte formation was consistent for all mice at 12 and 16 weeks, regardless of injury mode. Specifically, there was considerable osteophyte formation on the anterior-medial aspect of the distal femur, the menisci (particularly the medial meniscus) exhibited hypertrophy and osteophyte formation, primarily extending in an anteromedial direction from the joint (Fig. 5). The posterior medial tibial plateau exhibited bone formation in the posterior direction, and extreme erosion of the tibial plateau was observable with μCT, exposing the underlying subchondral bone.

Both injury models exhibited increased osteophyte volume from 12 to 16 weeks, although this increase was only significant for the Low Speed injury group (Fig. 6). The High Speed injury group exhibited higher osteophyte volume compared to the low speed injury group at both time points; this difference was statistically significant at 12 weeks ($p = 0.04$). We were able to observe preliminary signs of osteophyte formation on transverse μCT images of injured joints as early as 10 days post-injury, particularly on the anteromedial aspect of the distal femur (Fig. 5).

Anterior-Posterior Joint Laxity

We observed a greater than 2-fold increases in anterior-posterior (AP) joint laxity immediately following joint injury with both injury modes (Fig 7). We observed no significant difference in joint laxity between flexion angles for any group at any time point. By 12 and 16 weeks post-injury, AP joint laxity for both injured groups was reduced to control values. During AP laxity testing of week 16 legs, one control leg was broken during potting. Additionally, injured knees of week 16 mice had severely diminished range of motion and were difficult to extend to 30°. As a result, three of the 1 mm/s and two of the 500 mm/s week 16 knees were also fractured. 30° extension was tested last to ensure that data was collected for 60° and 90° joint angles.

No change in joint laxity was observed for day 0 uninjured joints after fixation in 4% paraformaldehyde and preservation in 70% ethanol for 4 weeks (compared to fresh-frozen joints), but injured joints exhibited significantly increased joint laxity after fixation (+18% AP joint laxity). Subsequently, joint laxity values of day 0 preserved knees were used for all comparisons between day 0, week 12, and week 16 data.

Long Term Whole Joint Histology

Whole joint histology showed extreme degeneration and OA for both injury modes at 12 and 16 weeks post-injury (Fig. 8). OARSI scores were significantly higher than uninjured control (UIC) joints at 12 and 16 weeks for both injury modes, however there were no significant differences between High Speed and Low Speed injured joints (Fig. 9). Injured joints exhibited extreme erosion of cartilage on both the medial and lateral aspects of the tibia and femur. Many injured joints had bone-bone contact and even erosion of subchondral bone, sometimes extending as far as the growth plate. There was extreme fibrosis within the joint space and osteophytes present on the tibia and femur. The menisci on both sides were hypertrophied and degenerated. Inspection of individual sections showed the most severe degeneration on the posterior aspect of the tibial plateau of injured joints, while the anterior aspect appeared comparable to uninjured controls. At 16 weeks the UIC joints were given an average OARSI score of approximately 2, indicating mild OA occurring naturally in the mice by 26 weeks of age.

DISCUSSION

In this study we used a non-invasive injury model in mice to compare two similar but distinctly different injury modes, and assess potential differences in PTOA development. Using different tibial compression loading rates, we were able to produce two unique injury modes in the knees of mice: ACL rupture with avulsion fracture ("Low Speed injury", 1 mm/s loading rate) or midsubstance ACL rupture ("High Speed injury", 500 mm/s loading rate). Consistent with our hypothesis, we found that the two injury modes were not significantly different from each other with respect to long-term changes in bone structure, joint laxity, and cartilage degeneration. However, we observed a greater loss of trabecular bone in the distal femoral epiphysis at 10 days post-injury in the Low Speed injury model compared to High Speed injury. This difference is likely due to direct bone damage caused by avulsion of the ACL in the Low Speed injury group. We also observed significant differences in osteophyte formation, with High Speed injured knees developing greater osteophyte volume. Altogether, these results suggest that ACL injury mode in mice is a minor contributing factor to the subsequent joint degeneration that follows traumatic joint injury after 12–16 weeks.

The role of subchondral bone in progression of OA has been an active topic of discussion [16–18], with authors hypothesizing that cartilage health is influenced by the structure of the underlying subchondral bone. However, early changes in subchondral bone and epiphyseal trabecular bone are not well defined in human subjects, but rather established (severe) OA is typically studied [19]. A few recent studies have investigated epiphyseal trabecular bone changes in the knees of osteoarthritic subjects using MRI imaging [20, 21], and have

observed decreased trabecular bone parameters (loss of trabecular bone) in osteoarthritic knees, particularly in the lateral compartment. This is consistent with the current study and our previous study [8] that showed trabecular bone loss from both the medial and lateral compartments in mice, although our previous study found similar magnitudes of trabecular bone loss from the medial and lateral compartments. Subchondral bone sclerosis and osteophyte formation are also common findings in humans with OA [22]. This is consistent with the current study, in which we observed thickening of the tibial subchondral bone plate, and considerable osteophyte formation around the joint by 12 and 16 weeks post-injury. The relatively large scale of osteophytes observed in this study is not typical for OA in humans, although this may be due to the fact that bone features do not scale linearly with body size between mice and humans. For example, body mass in humans is approximately 2000–4000 times greater than that of mice, while trabecular thickness in humans is approximately 4–7 times greater (100–350 μm in humans vs. 25–50 μm in mice). Altogether, the subchondral and trabecular bone changes observed in this mouse model of PTOA are generally consistent with the bone changes observed in human OA.

By both 12 and 16 weeks post-injury we observed severe OA in injured knees. This is in contrast to our previous study, in which joints exhibited only mild OA by 8 weeks post-injury, with loss of Safranin-O staining, minor fissuring, and cell death in the superficial zone [8]. In the current study we found that by only 4 weeks later (12 weeks post injury), injured joints exhibited severe OA with total loss of cartilage tissue. In many joints there was bone on bone contact, extreme fibrosis, and severe meniscal degeneration visible by 12 weeks post-injury, often to a degree that is unnecessary for studies of arthritis development. The severe posterior bone erosion we observed on the tibial plateau, particularly on medial side, is not typical of ACL injury-induced PTOA in other animal species or in humans, although similar erosion has been described with surgical transection of the ACL in mice [4]. This posterior degeneration may therefore be specific to mouse models of ACL-induced PTOA irrespective of how the ACL is ruptured (with or without surgery). In this way, ACL injury in mice may be limited for translation to human injuries. For future studies with this model, we anticipate that an 8–10 week end point should be sufficient to show moderate to severe OA, and would be sufficient to detect any improvement in OA development due to treatment. In contrast, the DMM and ACLT models utilized by Glasson et al. [4] were able to induce moderate-to-severe OA by 4 weeks post-injury.

Changes in AP joint laxity of injured knees in this study were similar to values obtained from previous studies using C57BL/6 mice with healthy knees. At ±0.8 N in healthy ACL intact joints, Blankevoort et al. [14] measured 0.43±0.16 mm and Wang et al. [13] measured 0.50±0.09 mm, compared to 0.57±0.08 mm in our study. The increased joint laxity measured in this study is likely due to the additional degree of freedom in our test fixture, which allowed rotation of the tibia about its longitudinal axis. The previous studies only allowed two degrees of freedom of motion.

In this study we observed consistent and repeatable patterns of osteophytosis around the joint capsule by 12 and 16 weeks post injury for both injury modes. In particular, we observed osteophytes forming from the anteriomedial femur, the posteromedial tibia, and the medial meniscus. It is possible that osteophyte formation around the joint may have

contributed to the reduction in joint laxity from day 0 values. The stabilizing effect of osteophytes in osteoarthritic joints was previously studied by Pottenger et al. in humans undergoing total knee arthroplasty (TKA) by measuring varus-valgus (VV) laxity before and after removal of osteophytes [23]. They observed an increase in VV joint laxity from 11.0° to 14.7° after osteophyte removal, showing that osteophytes helped stabilize the joint. These results support the hypothesis that osteophytes form as a response to joint instability. The drawback to restoring joint stability by osteophyte formation is severe reduction in joint range of motion, which was observed in the current study. 12- and 16-week knees were extremely stiff and resisted extension to 30°. This is supported by a study in humans undergoing TKA, in which residual posterior femoral condyle osteophytes were associated with reduced knee flexion after surgery. Removal of the osteophytes avoided impingement with the implant and allowed more flexion to occur [24]. Unfortunately, our study did not investigate AP joint laxity at intermediate time points between 0 and 12 weeks post-injury. Future analyses could investigate the time course of "re-stabilization" of the joint after ACL rupture, and could confirm the proposed correlation with osteophyte formation.

Future studies using this model should include additional biomechanical analyses to further characterize relationships between joint injury and OA progression. Gait analysis of injured mice could address questions concerning voluntary mechanical loading after injury and whether mice change limb-loading patterns. If the mice are unweighting the injured limb, then loss of bone volume may be partly explained due to disuse. Additionally, future studies could investigate the activity level of mice following joint injury. It is possible that voluntary cage activity is reduced, which would result in further mechanical loading-related bone atrophy. The opposite is also likely true; increased cage activity or exercise (including fighting) could exacerbate PTOA progression following injury.

This study advances our previous study by analyzing multiple injury modes, quantifying biomechanical changes in the joint, and analyzing time points at which severe OA is present. However, there are still limitations that must be acknowledged. In particular, while anatomical structures between human and mice are similar, the bipedal gait of humans is very different from that of mice, and may result in divergent laxity changes, loading patterns, and locations of degeneration. Additionally, the severe osteophyte formation that we observe with this model is not typical for human joints, although it is comparable to other widely used mouse models [25], and may be largely explained by the dramatic size difference between mouse and human joints. Finally, these studies used 10 week-old mice with open growth plates (the growth plates in mouse long bones typically remain open throughout the lifetime of the animal). This is a ubiquitous limitation of using mice for studies of bone, and may have contributed to the skeletal adaptation observed in this study. While this model may not be able to overcome all of these limitations, it still has several advantages over other existing mouse models of PTOA, and may be uniquely useful for investigating OA progression in humans.

In conclusion, in this study we found that ACL injury mode does not affect the long term bone changes or OA severity in mice, although it does affect short term trabecular bone turnover, with injury involving direct bone damage (avulsion) exhibiting greater short term trabecular bone loss. We also found that ACL injury dramatically increased anterior-

posterior joint laxity in mice immediately following injury, but joint stability is restored by 12 weeks post-injury, possibly due to extensive osteophyte formation around the joint. These studies further characterize the non-invasive knee injury mouse model developed in our lab, and begin to describe mechanical loading changes initiated by joint injury. The model presented provides an opportunity to explore fundamental questions regarding the role of bone turnover in PTOA progression, and findings from this model may point to bone turnover as a potential target for therapies aimed at slowing or preventing PTOA.

Acknowledgments

References

1. Felson DT. Epidemiology of hip and knee osteoarthritis. Epidemiol Rev. 1988; 10:1–28. [PubMed: 3066625]

2. Lohmander LS, Englund PM, Dahl LL, Roos EM. The long-term consequence of anterior cruciate ligament and meniscus injuries: osteoarthritis. Am J Sports Med. 2007; 35(10):1756–69. [PubMed: 17761605]

3. Oiestad BE, Engebretsen L, Storheim K, Risberg MA. Knee osteoarthritis after anterior cruciate ligament injury: a systematic review. Am J Sports Med. 2009; 37(7):1434–43. [PubMed: 19567666]

4. Glasson SS, Blanchet TJ, Morris EA. The surgical destabilization of the medial meniscus (DMM) model of osteoarthritis in the 129/SvEv mouse. Osteoarthritis Cartilage. 2007; 15(9):1061–9. [PubMed: 17470400]

5. Furman BD, Strand J, Hembree WC, Ward BD, Guilak F, Olson SA. Joint degeneration following closed intraarticular fracture in the mouse knee: a model of posttraumatic arthritis. J Orthop Res. 2007; 25(5):578–92. [PubMed: 17266145]

6. van Beuningen HM, Glansbeek HL, van der Kraan PM, van den Berg WB. Osteoarthritis-like changes in the murine knee joint resulting from intra-articular transforming growth factor-beta injections. Osteoarthritis Cartilage. 2000; 8(1):25–33. [PubMed: 10607496]

7. Poulet B, Hamilton RW, Shefelbine S, Pitsillides AA. Characterising a novel and adjustable non-invasive murine knee joint loading model. Arthritis Rheum. 2011; 63(1):137–47. [PubMed: 20882669]

8. Christiansen BA, Anderson MJ, Lee CA, Williams JC, Yik JH, Haudenschild DR. Musculoskeletal changes following non-invasive knee injury using a novel mouse model of post-traumatic osteoarthritis. Osteoarthritis Cartilage. 2012; 20(7):773–82. [PubMed: 22531459]

9. Gottsegen CJ, Eyer BA, White EA, Learch TJ, Forrester D. Avulsion fractures of the knee: imaging findings and clinical significance. Radiographics. 2008; 28(6):1755–1770. [PubMed: 18936034]

10. Crowninshield RD, Pope MH. The strength and failure characteristics of rat medial collateral ligaments. The Journal of Trauma. 1976; 16(2):99–105. [PubMed: 1255835]

11. Noyes FR, DeLucas JL, Torvik PJ. Biomechanics of anterior cruciate ligament failure: An analysis of strain-rate sensitivity and mechanisms of failure in primates. J bone Joint Surg Am. 1976; 56(2):236–253. [PubMed: 4452684]

12. Bouxsein ML, Boyd SK, Christiansen BA, Guldberg RE, Jepsen KJ, Muller R. Guidelines for assessment of bone microstructure in rodents using micro-computed tomography. Journal of bone and mineral research: the official journal of the American Society for Bone and Mineral Research. 2010; 25(7):1468–86.

13. Wang VM, Banack TM, Tsai CW, Flatow EL, Jepsen KJ. Variability in tendon and knee joint biomechanics among inbred mouse strains. Journal of orthopaedic research: official publication of the Orthopaedic Research Society. 2006; 24(6):1200–7. [PubMed: 16705702]

14. Blankevoort L, van Osch JVM, Janssen B, Hekman EEG. In vitro laxity-testers for knee joints of mice. J Biomechanics. 1996; 29(6):799–806.

15. Glasson SS, Chambers MG, Van Den Berg WB, Little CB. The OARSI histopathology initiative - recommendations for histological assessments of osteoarthritis in the mouse. Osteoarthritis and cartilage/OARS, Osteoarthritis Research Society. 2010; 18 (Suppl 3):S17–23.

16. Mansell JP, Tarlton JF, Bailey AJ. Biochemical evidence for altered subchondral bone collagen metabolism in osteoarthritis of the hip. Br J Rheumatol. 1997; 36(1):16–19. [PubMed: 9117167]

17. Hayami T, Pickarski M, Zhuo Y, Wesolowski GA, Rodan GA, Duong le T. Characterization of articular cartilage and subchondral bone changes in the rat anterior cruciate ligament transection and meniscectomized models of osteoarthritis. Bone. 2006; 38(2):234–43. [PubMed: 16185945]

18. Radin EL, Rose RM. Role of subchondral bone in the initiation and progression of cartilage damage. Clinical Orthopaedics and Related Research. 1986 Dec.(213):34–40. [PubMed: 3780104]

19. Mastbergen SC, Lafeber FP. Changes in subchondral bone early in the development of osteoarthritis. Arthritis Rheum. 2011; 63(9):2561–3. [PubMed: 21360518]

20. Chiba K, Uetani M, Kido Y, Ito M, Okazaki N, Taguchi K, Shindo H. Osteoporotic changes of subchondral trabecular bone in osteoarthritis of the knee: a 3-T MRI study. Osteoporos Int. 2011; 23(2):589–97. [PubMed: 21359670]

21. Bolbos RI, Zuo J, Banerjee S, Link TM, Ma CB, Li XJ, Majumdar S. Relationship between trabecular bone structure and articular cartilage morphology and relaxation times in early OA of the knee joint using parallel MRI at 3 T. Osteoarthritis and Cartilage. 2008; 16(10):1150–1159. [PubMed: 18387828]

22. Jacobson JA, Girish G, Jiang Y, Sabb BJ. Radiographic evaluation of arthritis: degenerative joint disease and variations. Radiology. 2008; 248(3):737–47. [PubMed: 18710973]

23. Pottenger LA, Phillips FM, Draganich LF. The effect of marginal osteophytes on reduction of varus–valgus instability in osteoarthritic knees. Arthritis Rheum. 1990; 33(6):853–858. [PubMed: 2363739]

24. Yau WP, Chiu KY, Tang WM, Ng TP. Residual posterior femoral condyle osteophyte affects the flexion range after total knee replacement. International orthopaedics. 2005; 29(6):375–9. [PubMed: 16167157]

25. Moodie JP, Stok KS, Muller R, Vincent TL, Shefelbine SJ. Multimodal imaging demonstrates concomitant changes in bone and cartilage after destabilisation of the medial meniscus and increased joint laxity. Osteoarthritis and cartilage/OARS, Osteoarthritis Research Society. 2011; 19(2):163–70.
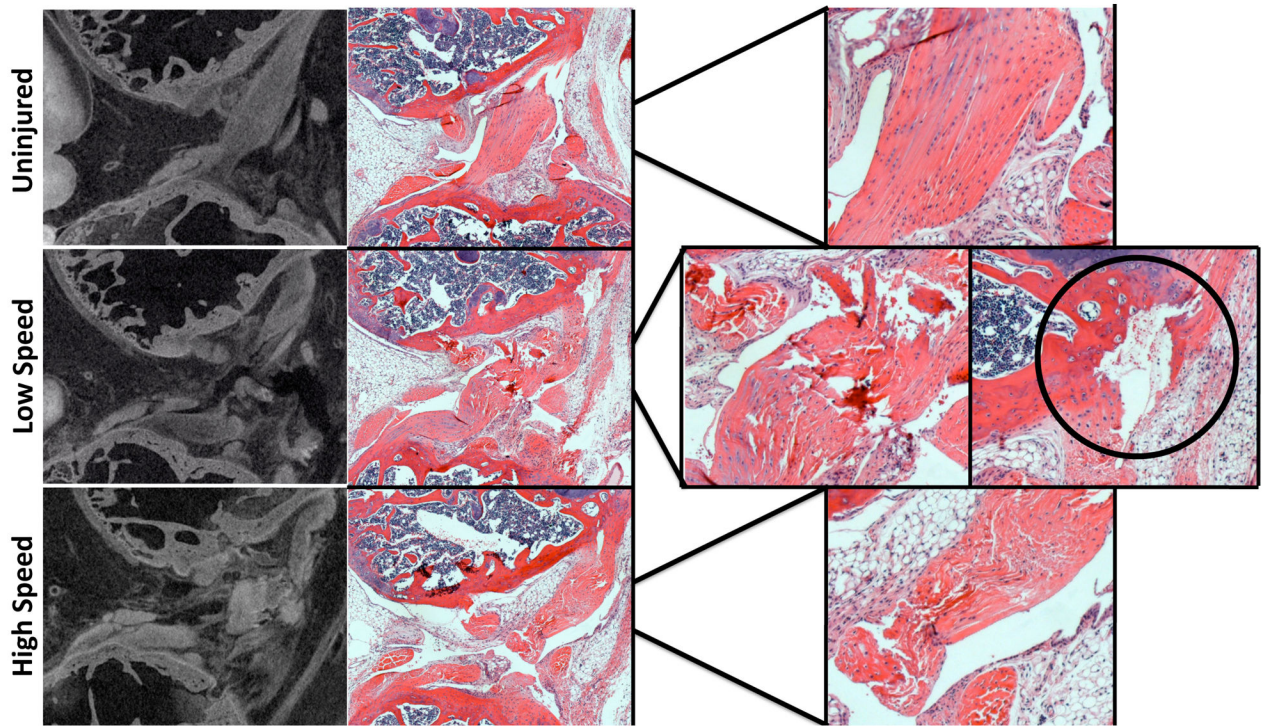
Figure 1.
Imaging of injured and uninjured knee joints. Contrast-enhanced µCT images (left column) show disruption of the ACL in both High Speed and Low Speed injuries. Hemotoxylin and Eosin sections of intact, High Speed, and Low Speed injury modes (middle and right columns) show disruption of the ACL with both injury modes compared to uninjured ligament. Low Speed injury (1 mm/s) caused avulsion of the ACL from the posterior femur (circle). No avulsion was detected in the High Speed (500 mm/s) injury group.
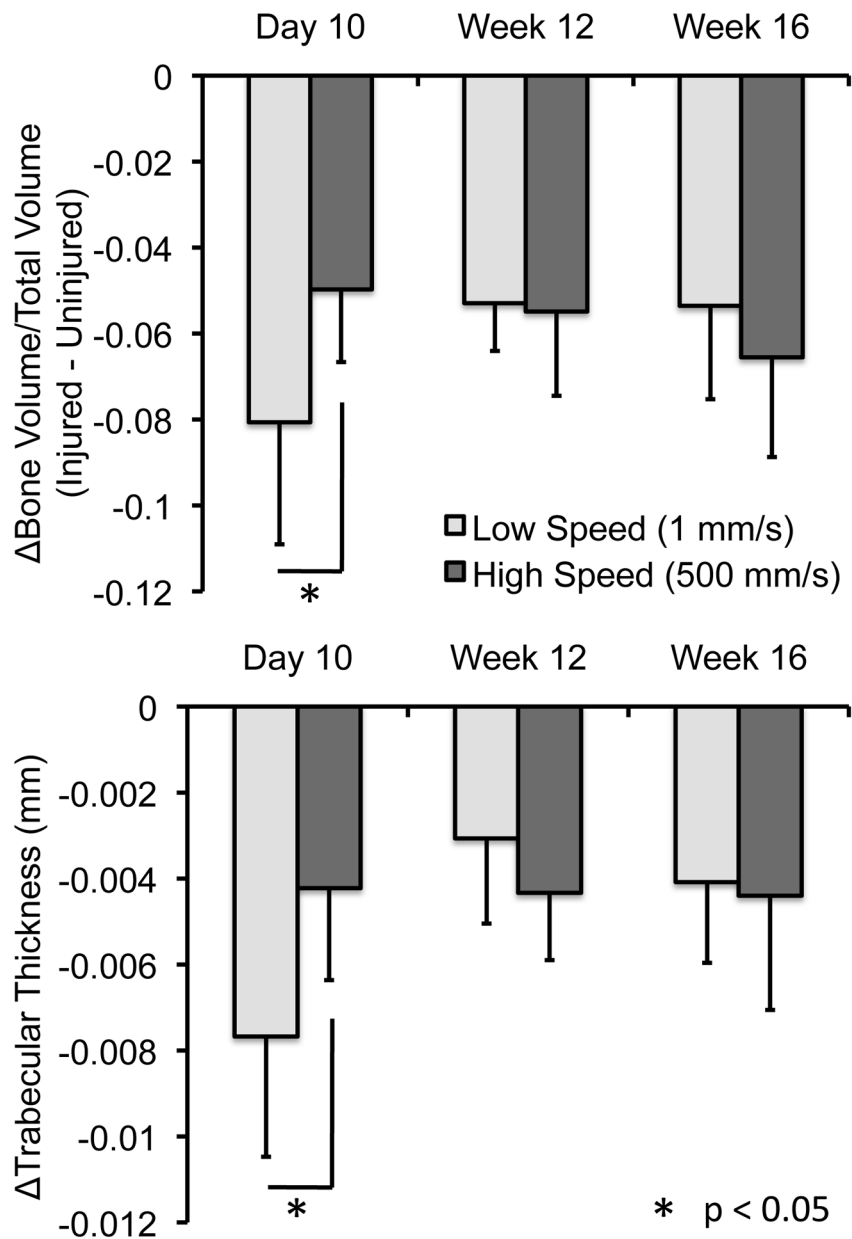
Figure 2.
Difference in bone volume fraction (BV/TV) and trabecular thickness (Tb.Th) of the distal femoral epiphyses for Low Speed (1 mm/s) and High Speed (500 mm/s) injury groups. Values are the average difference between injured and contralateral control legs for each mouse. Injured vs. uninjured values were significantly different for all groups and all time points ($p < 0.05$). Mice injured at Low Speed, which induced avulsion from the distal femur, exhibited greater trabecular bone loss at 10 days post-injury. After 12–16 weeks, injured knees still had significantly reduced bone volume and trabecular thickness compared to uninjured knees, although there were no differences between High Speed and Low Speed injuries in trabecular structure at these time points.
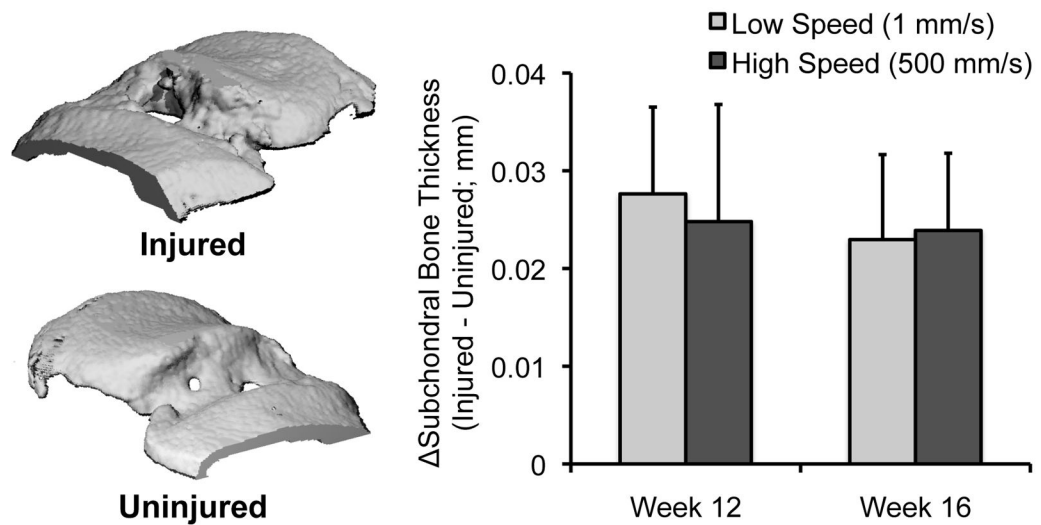
Figure 3.
(Left) Micro-computed tomography reconstructions of the subchondral bone plate of the tibial plateau of injured and uninjured knees, with a medial cut for visualization of subchondral bone thickness. (Right) Difference in subchondral bone thickness of the proximal tibial plateau for Low Speed (1 mm/s) and High Speed (500 mm/s) injury groups. Values are the average difference between injured and contralateral control legs for each mouse. Injured vs. uninjured values were significantly different for all groups and all time points (p < 0.05). No significant differences were observed between injury modes or time points.
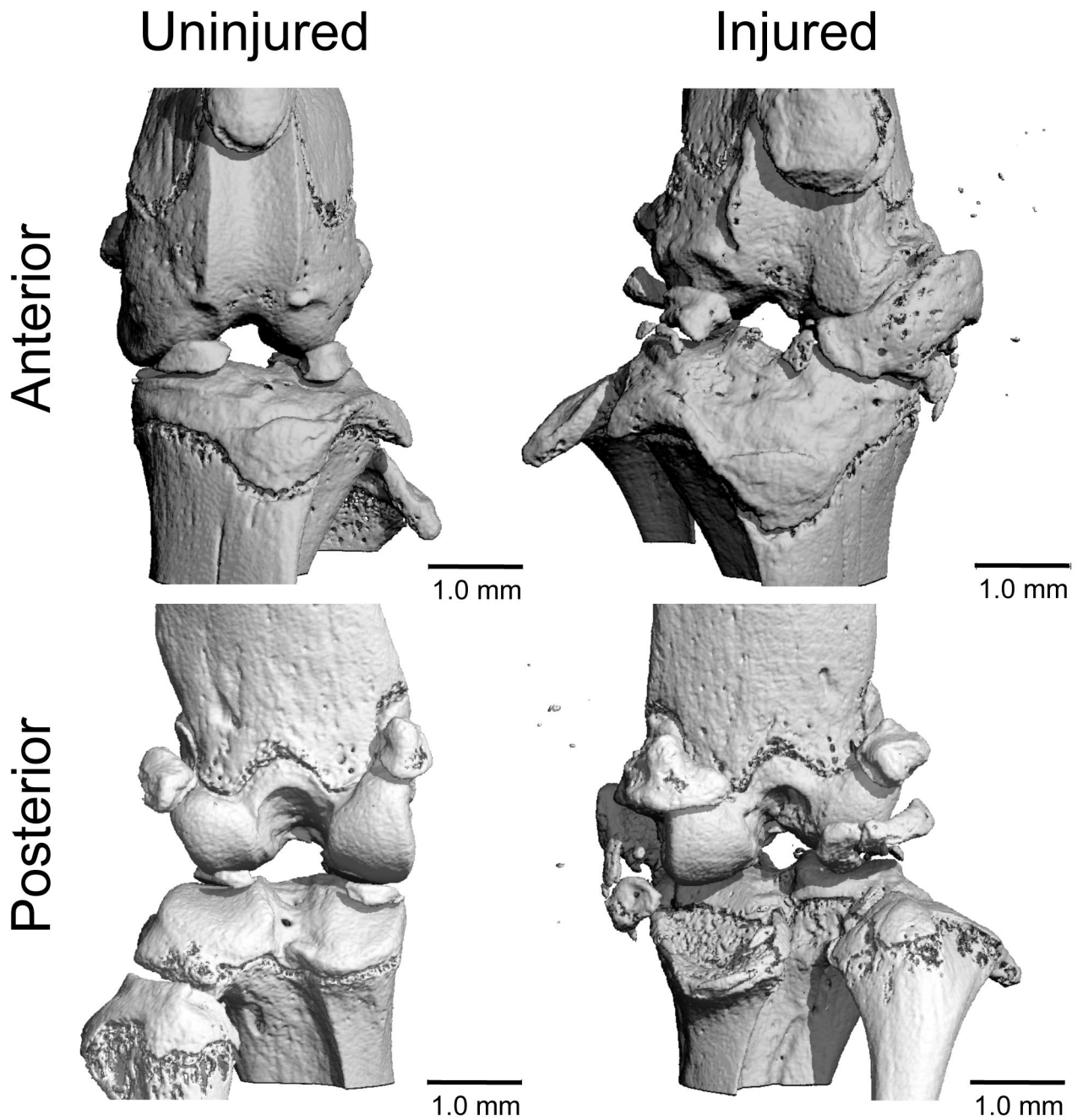
Figure 4.
μCT images of injured and uninjured mouse knees at 12 weeks post-injury (Low Speed injury). Substantial osteophytosis and joint degeneration were observed in all injured knees. In particular, osteophytes were observed on the anteriomedial aspect of the distal femur, the posteromedial aspect of the proximal tibia, and the medial meniscus.
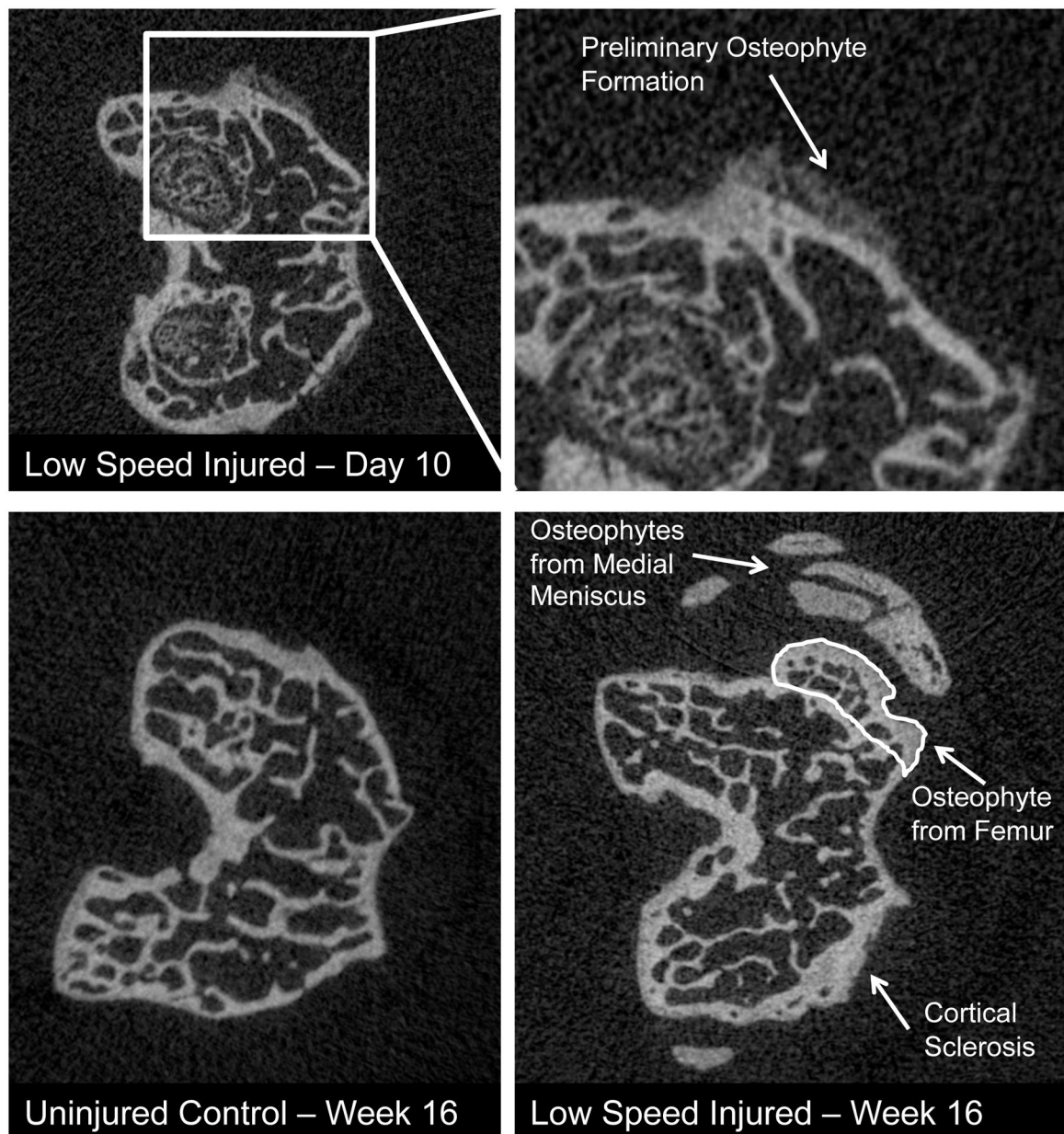
Preliminary Osteophyte Formation

Low Speed Injured – Day 10

Osteophytes from Medial Meniscus

Osteophyte from Femur

Cortical Sclerosis

Uninjured Control – Week 16

Low Speed Injured – Week 16

Figure 5.
Transverse μCT slices of the distal femur. Top: Femoral epiphysis of an injured joint 10 days post-injury, with expanded image showing early osteophytosis from the anteriomedial femur. Bottom: Uninjured (left) and injured (right) femoral epiphysis at 16 weeks showing considerable osteophyte formation from the anteriomedial femur and medial meniscus, as well as sclerosis of cortical plate on the lateral condyle.
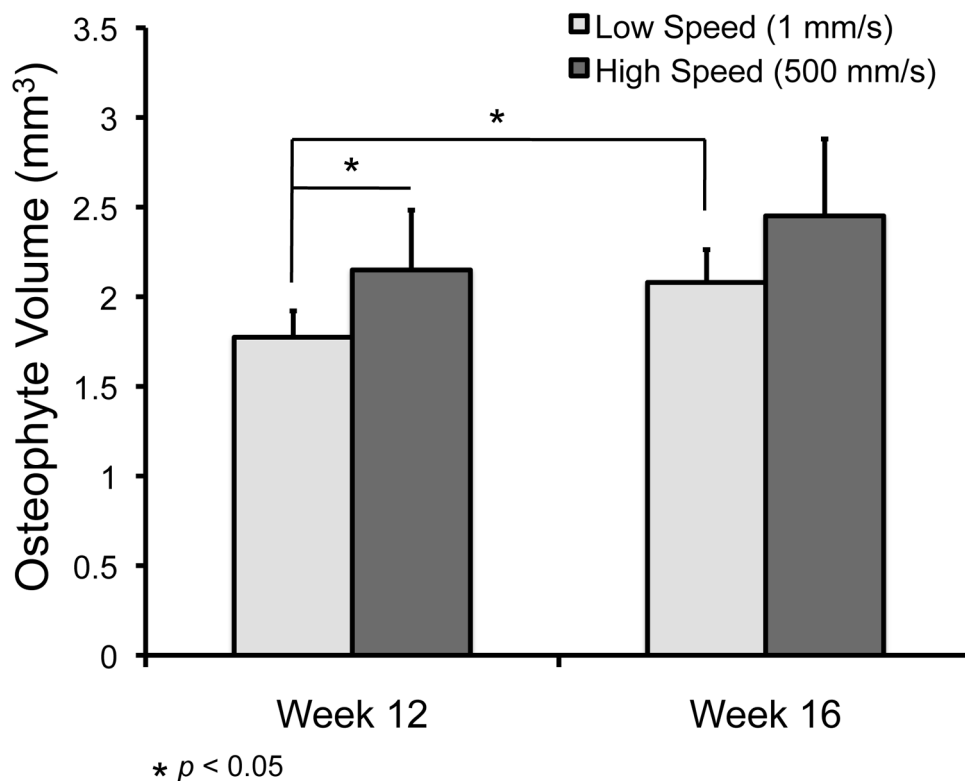
Figure 6.
Osteophyte volume of injured joints. Non-native bone formation was quantified for Low Speed (1 mm/s) and High Speed (500 mm/s) injured joints at 12 and 16 weeks post-injury. High Speed injured joints exhibited greater osteophyte volume than Low Speed injured joints at 12 weeks post-injury. Osteophyte volume increased from 12 to 16 weeks for both groups, but this increase was only significant for Low Speed injured mice ($p < 0.05$).
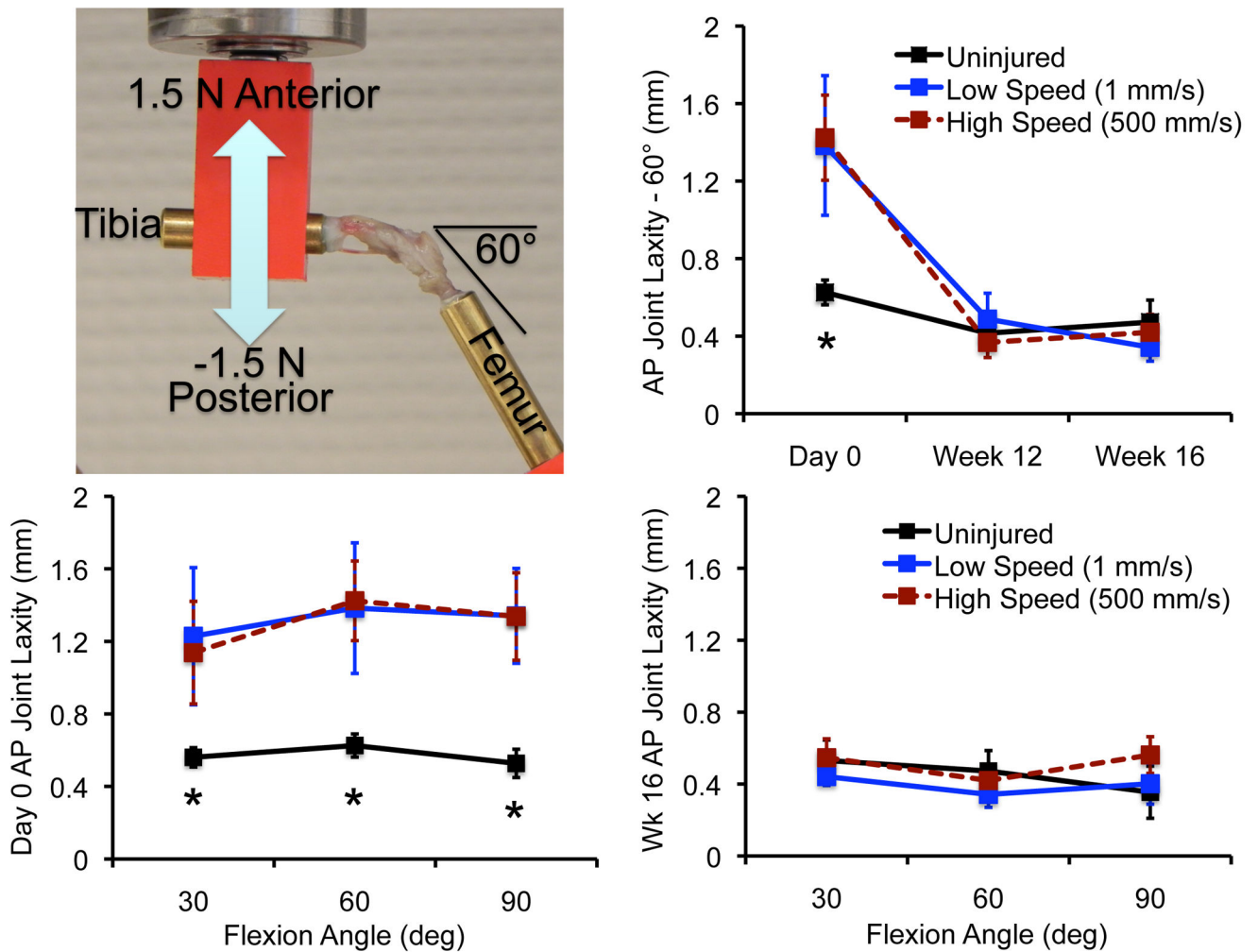
Figure 7.
Top left: Joint laxity test setup for 60° of flexion. Top right: Total anterior-posterior joint laxity at 60° for day 0, week 12, and week 16 knees. * p < 0.05 between injured and uninjured values. Injured joints had a greater than 2-fold increase in joint laxity at day 0, but joint stability was returned to control values by 12 and 16 weeks post-injury. Bottom: Total anterior-posterior joint laxity at day 0 (left) and week 16 (right) at 30°, 60°, and 90° of knee flexion. *p < 0.05 between injured and uninjured values. There were no significant differences between joint angles, or between injury modes (High Speed vs. Low Speed injury).
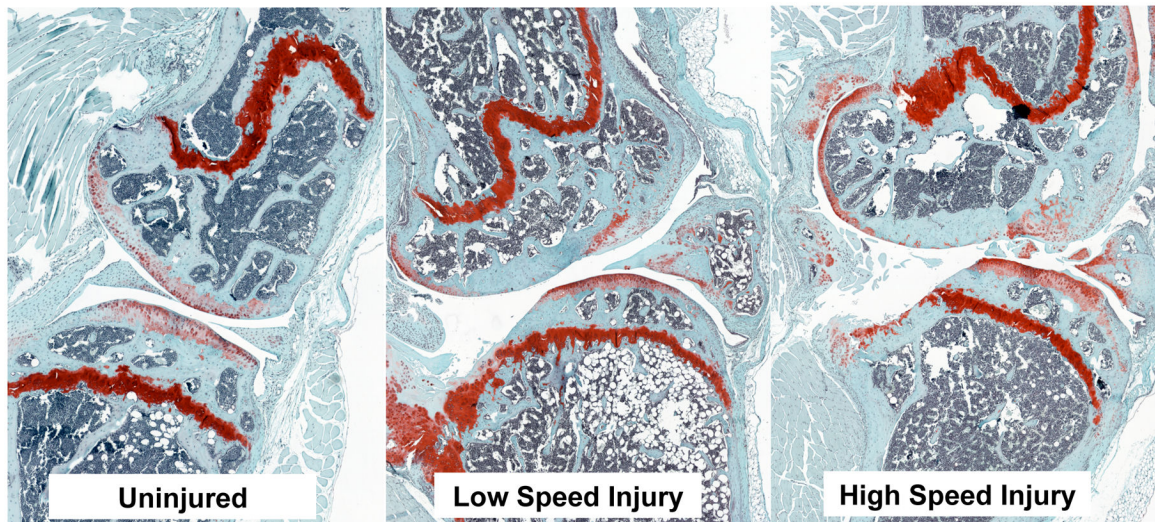
Figure 8.
Whole joint histology at 12 weeks. Sagittal sections of the medial condyle stained with Safranin-O and Fast Green. By 12 weeks post-injury we observed significant degeneration of both the tibia and femur. In particular, the posterior aspect of the medial tibia has severe degeneration of cartilage and bone erosion, often extending as far as the growth plate.
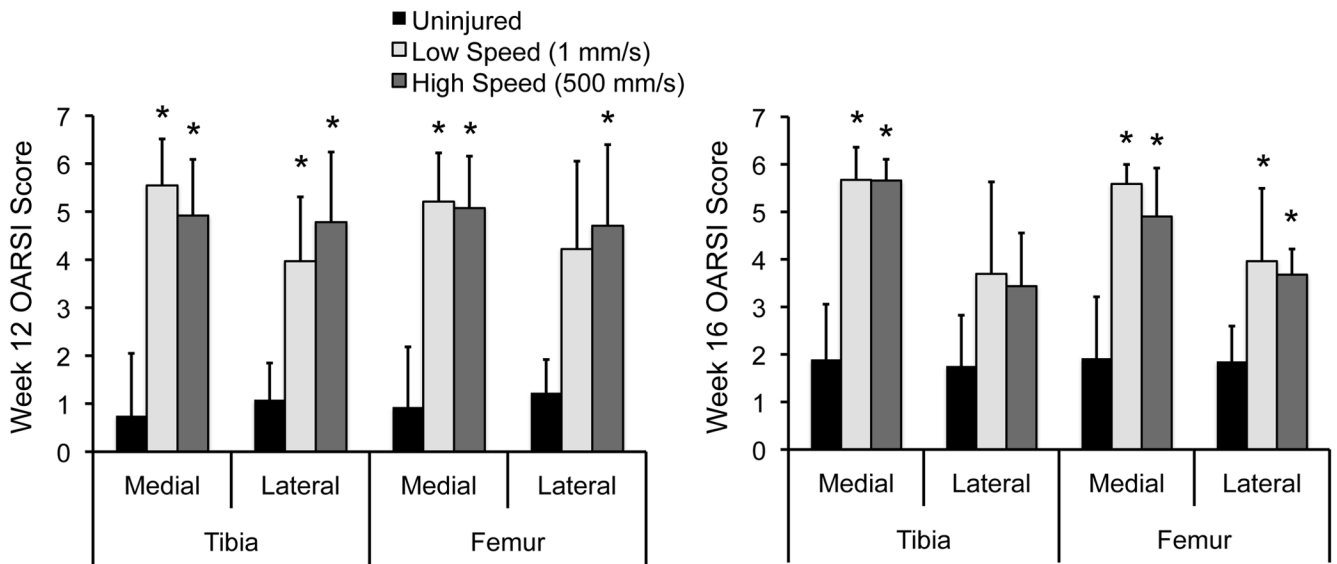
Figure 9.
OARSI scores for whole joint histology at 12 and 16 weeks. We observed severe osteoarthritis of both the tibia and femur at both time points, often with degeneration of articular cartilage extending to the subchondral bone (* indicates significant difference from uninjured control. No statistically significant differences were observed in the OARSI score of knees injured with the High Speed versus Low Speed injury mode).

Table 1

Animal numbers and experimental groups for "Comparison of High Speed and Low Speed Injury Models".

Time Point	Low Speed	High Speed	Sham
Day 0	6	6	
Day 10	8	8	6
Week 12	6	6	3
Week 16	6	6	3